doi:10.20944/preprints201806.0294.v1

Peer-reviewed version available at *Molecules* **2018**, *23*, 1732; doi:10.3390/molecules23071732

Article

Synthesis of nitrogen-rich polymers by click polymerization reaction and gas sorption property

Jingru Song [1,2,*], Wengui Duan [1,*], Dianpeng Li [2]

[1] School of Chemistry & Chemical Engineering of Guangxi University, Nanning, Guangxi, China; songjingru@iccas.ac.cn
[2] Guangxi Institute of Botany, Chinese Academy of Sciences, Guilin, Guangxi, China; ldp@gxib.cn
* Correspondence: songjingru@iccas.ac.cn (J. S.); wgduan@gxu.edu.cn (W. D.); Tel.: +86-771-323-9910 (W. D.)

Abstract: Microporous organic polymers (MOPs) are promising materials for gas sorption because of the intrinsic and permanent porosity, designable framework and low density. The introduction of nitrogen-rich building block in MOPs will greatly enhance the gas sorption capacity. Here, we report the synthesis of MOPs from the 2,4,6-tris(4-ethynylphenyl)-1,3,5-triazine unit and aromatic azides linkers via click polymerization reaction. FTIR and solid state ^{13}C CP-MAS NMR confirm the formation of the polymers. CMOP-1 and CMOP-2 exhibit microporous networks with BET surface area of 431 and 406 m^2 g^{-1} and narrow pore size distribution under 1.2 nm. Gas sorption isotherms including CO_2 and H_2 were measured. CMOP-1 stores superior CO_2 level of 8.2 wt% (1.88 mmol g^{-1}) at 273 K/1.0 bar and H_2 uptake up to 0.6 wt% at 77 K/1.0 bar, while CMOP-2 with smaller surface area shows lower CO_2 adsorption capacity of 7.3 wt% (1.66 mmol·g^{-1}) and H_2 uptake (0.5 wt%). In addition, I_2 vapor adsorption was tested at 353 K. CMOP-1 shows higher gravimetric load of 160 wt%. Despite of the moderate surface area, the CMOPs display excellent sorption ability for CO_2 and I_2 due to the nitrogen-rich content in the polymers.

Keywords: microporous organic polymers; nitrogen-rich; CO_2 adsorption; H_2 adsorption; I_2 vapor sorption

---

1. Introduction

During the last few decades, microporous organic polymers (MOPs) have been intensively investigated and applied in various fields such as heterogeneous catalysis [1], gas adsorption and separation [2-3], adsorption of radioactive iodine [4], drug delivery [5-6] and photovoltaics [7-9] duo to the low density, large surface area, high thermal/chemical stability, functional surface and diverse building blocks. Until now, numerous MOPs including crystalline covalent organic frameworks (COFs) [10], covalent triazine frameworks (CTFs) [11], benzimidazole-linked polymers (BILPs) [12], porous polymer networks (PPNs) [13], hyper-crosslinked polymers (HCPs) [14], conjugated microporous polymers (CMPs) [15], polymers of intrinsic microporousity (PIMs) [16] and porous aromatic frameworks (PAFs) [17] have been synthesized via different polymerization reactions and versatile synthons. Amorphous polymers have received more and more attention owing to the tunable pore size, high stability and controllable reaction than crystalline networks.

The excessive emission of carbon dioxide is believed the mainly contribution to the global warming problem resulting from the burning of fossil fuels. Great effort has been devoted to exploring the technology for CO_2 capture and storage. Recently, MOPs have generated enormous interest in the area of gas sorption for carbon dioxide, hydrogen, iodine and methane because of their low weigh and remarkable microporous framework [18-20]. To achieve higher gas uptake by MOPs, large surface area, suitable pore size and strong interaction are crucial and desired. The introduction of heteroatom especially nitrogen or oxygen has been demonstrated to be feasible and effective to enhance adsorption load by means of stronger interaction between gas molecule and adsorbent [21-23]. Triazine-based building blocks which have inherent nitrogen atom can not only combine metal ions for catalysis [24] but also provide polarizable sites for gas uptake. Pan *et al.*

Peer-reviewed version available at *Molecules* **2018**, *23*, 1732; doi:10.3390/molecules23071732

reported imide functionalized 1,3,5-triazine frameworks named TPIs@IC. The polymers had ultramicropores at 5.4-6.8 Å which can adsorb 3.2 mmol g^{-1} CO_2 (273 K/1 bar) and 1.47 wt% H_2 (77 K/1 bar) [25]. Bu *et al.* synthesized aminal-linked porous organic polymers APOPs with a moderate specific surface area (S_{BET}=724-1402 m^2 g^{-1}) but significant gas adsorption (CO_2: 4.54 mmol g^{-1} at 273 K/1 bar; H_2: 8.95 mmol g^{-1} at 77 K/1 bar), especially high CO_2 adsorption and good selectivity over N_2 at low pressure (0.15 bar) [26]. In 2015, Lotsch *et al.* reported amorphous CTFs synthesized at different temperature. For these polymers, excellent CO_2 (5.58 mmol g^{-1}) and H_2 (2.12 wt %) adsorption capacities were observed [27]. In addition, many CIFs with microporous framework for gas storage and separation have been reported such as the cCTF (S_{BET}=1247 m^2 g^{-1}; CO_2: 13.3 wt%), *fl*-CTFs (S_{BET}=15-2862 m^2 g^{-1}; CO_2: 1.27-4.28 mmol g^{-1}), CTF-TB-3 (S_{BET}=612 m^2 g^{-1}; CO_2: 16.84 wt%) and CTF-BIs (CO_2: 21.68 wt%) [28-31]. Zhang *et al*. synthesized polymers with N-heterocyclic groups (NAPOPs). NAPOP-1 and NAPOP-3 exhibit high adsorption toward iodine (>240 wt%) and moderate CO_2 adsorption [32]. Geng *et al.* constructed novel triazine-based TCMPs by Friedel-Crafts polymerization reaction [33]. Among them, TTPPA displays excellent reversible iodine vapor uptake of 4.90 g g^{-1}. Furthermore, the TCMPs show sensitive sensing ability towards *o*-nitrophenol.

The N-heterocycle derived from the efficient click reaction can further increase the nitrogen content for abundant sorption sites. Keep this consideration in mind, we synthesized nitrogen-rich polymers named CMOPs from 2,4,6-tris(4-ethynylphenyl)-1,3,5-triazine (TEPT) and azides by click polymerization reaction (Scheme 1). The polymers were characterized by FTIR, solid state ^{13}C CP-MAS NMR and elemental analysis (EA). Thermogravimetric analysis (TGA) showed the high thermal stability. Power X-ray diffraction (PXRD) and scanning electron microscopy (SEM) confirmed the amorphous but uniform phase. Nitrogen adsorption-desorption isotherms at 77 K were investigated to explore the surface area, porosity and pore size. In addition, adsorption measurements of CO_2, H_2 and I_2 were researched to evaluate the gas sorption capacity.

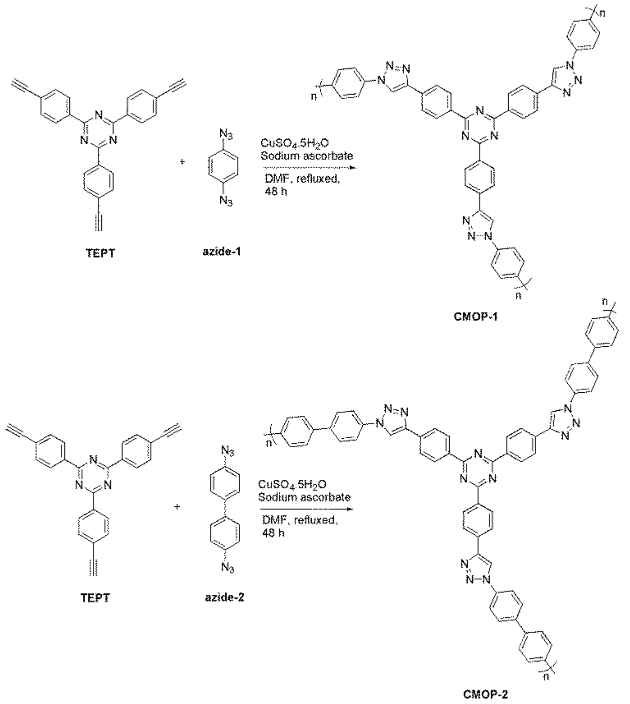

Scheme 1. The synthetic route to CMOPs.

2. Results

2.1. Synthesis and character

Peer-reviewed version available at *Molecules* **2018**, *23*, 1732; doi:10.3390/molecules23071732

The CMOPs were synthesized by click reaction in DMF solvent from TEPT and aromatic azides according to procedure in Scheme 1. The resulting brown powders were insoluble in common organic solvent such as tetrahydrofuran, dichloromethane, methanol, chloroform, acetone and *N*,*N*-dimethylformamide.

In the FTIR spectra of CMOPs (Figure S1), characteristic peaks for TEPT at 1505 and 3252 cm^{-1} attenuated dramatically, while peaks at 2106 and 2095 cm^{-1} for azide-1 and azide-2 disappeared, and new peaks at 1617, 2921 cm^{-1} for CMOP-1, 1612, 2927 cm^{-1} for CMOP-2 could be observed, confirming the occurring of click reaction and formation of triazole ring. The solid state ^{13}C CP-MAS NMR measurements gave similar spectra (Figure S2). The peak at 169 ppm could be attributed to carbon atom in triazine ring, while peak at 146 ppm was ascribed to phenyl carbon directly linked with triazine ring. The broad signals at about 131-110 ppm corresponded to the triazolyl and phenyl rings.

Thermogravimetric analysis in N_2 atmosphere showed that the polymers could keep thermal stability under 240 ^{o}C (CMOP-1) and 210 ^{o}C (CMOP-2). The first 5% weight loss was mainly due to the volatilization of solvent adsorbed in the polymers (Figure S3). Power X-ray diffraction (PXRD) analysis in the angle range of 5 to 35^{o} suggested the amorphous nature of the CMOPs which was because of the irreversibility of click reaction (Figure S4). Scanning electron microscopy (SEM) images revealed the phase purity with uniform morphology (Figure S5).

2.2. *Porosity*

The surface area and porosity of CMOPs was investigated by N_2 adsorption-desorption measurement at 77 K. The results were illustrated in Figure 1. CMOP-1 and CMOP-2 exhibited type-I isotherms which showed a sharp adsorption at relative low pressure ($P/P_o < 0.05$), indicating permanent microporous network. The Brunauer-Emmett-Teller (BET) surface areas were calculated to be 431 and 406 $m^2\ g^{-1}$, while microporous areas were 209 and 188 $m^2\ g^{-1}$. The total pore volumes of CMOP-1 and CMOP-2 were 0.458 and 0.387 $cm^3\ g^{-1}$, with 0.09 and 0.08 $cm^3\ g^{-1}$ microporous volume. The estimated pore sizes distribution on the basis of density functional theory (DFT) model were 0.6, 1.2 and 0.7, 1.2 nm for CMOP-1 and CMOP-2, consistent with the microporous N_2 sorption isotherm (Figure S6).

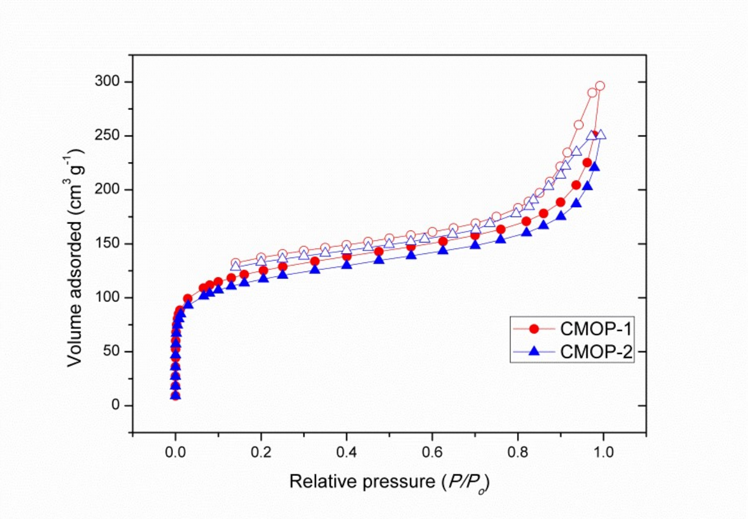

Figure 1. N_2 adsorption-desorption isotherm at 77 K (filled: adsorption; empty: desorption).

2.3. *Gas sorption capacity*

The microporous framework with narrow pore size distribution and nitrogen-rich character inspired us to explore CO_2 adsorption capacity. As shown in Figure 2, CMOP-1 exhibited higher CO_2 adsorption ability of 8.2 wt% at 273 K and 3.5 wt% at 298 K, while CMOP-2 with smaller surface area showed slightly lower uptake to 7.3 and 2.5 wt%, superior than many other

Peer-reviewed version available at *Molecules* **2018**, *23*, 1732; doi:10.3390/molecules23071732

heteroatom-rich polymers such as FPOP-1 (S_{BET}: 538 m² g⁻¹, 6.3 wt%), NOP-55 (S_{BET}: 526 m² g⁻¹, 8.6 wt%), CPOP-22 (S_{BET}: 440 m² g⁻¹, 6.9 wt%) and CuPor-BPDC (S_{BET}: 442 m² g⁻¹, 5.5 wt%) [34-37].

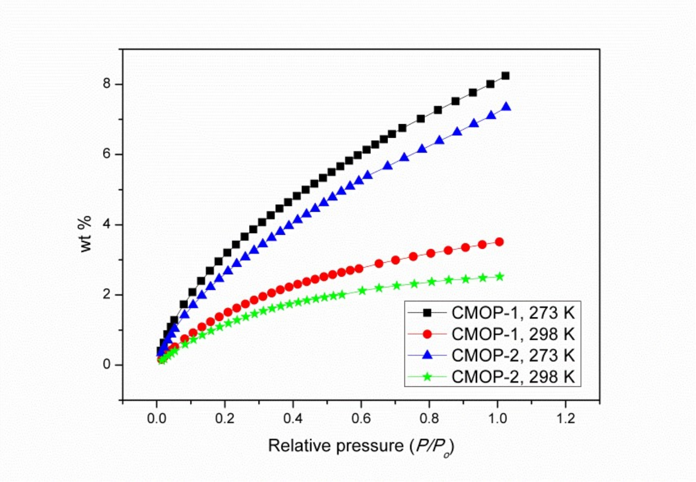

Figure 2. CO_2 adsorption isotherm at 273/298 K.

In addition, H_2 uptake was also investigated at 77 K (Figure 3). The adsorption capacity was increasing along with the pressure, and then up to saturation. The maximum uptakes were 0.6 and 0.5 wt% for CMOP-1 and CMOP-2. The moderate capacity originated from the low surface area.

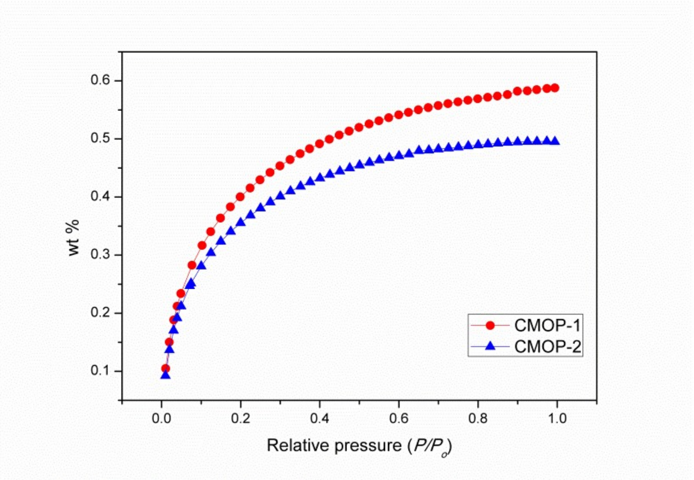

Figure 3. H_2 adsorption isotherm at 77 K.

It was found that nitrogen-rich polymer favored the sorption toward iodine owing to the stronger interaction between nitrogen atom and electron-deficient I_2 [4, 32-33]. The inserted images in Figure 4 showed the color change of I_2-cyclohexane (1 mg ml⁻¹) solution after adding 25 mg of CMOP-1 and CMOP-2. As time gone, the pink color of I_2-cyclohexane solution faded clearly, indicating the good removal efficiency. To evaluate the I_2 uptake ability of CMOPs, the sorption of I_2 vapor was investigated at 353 K. The solid powder was placed in an open bottle which was exposing to vapor of I_2 in a sealed container. As shown in Figure 4, the gravimetric uptake was gradually increasing, and then reached to the plateau after about 24 h. The sorption ability was 160 wt% and 93 wt% for CMOP-1 and CMOP-2. The larger capacity of CMOP-1 was mainly attributed to the larger surface area and more nitrogen atoms in the surface.

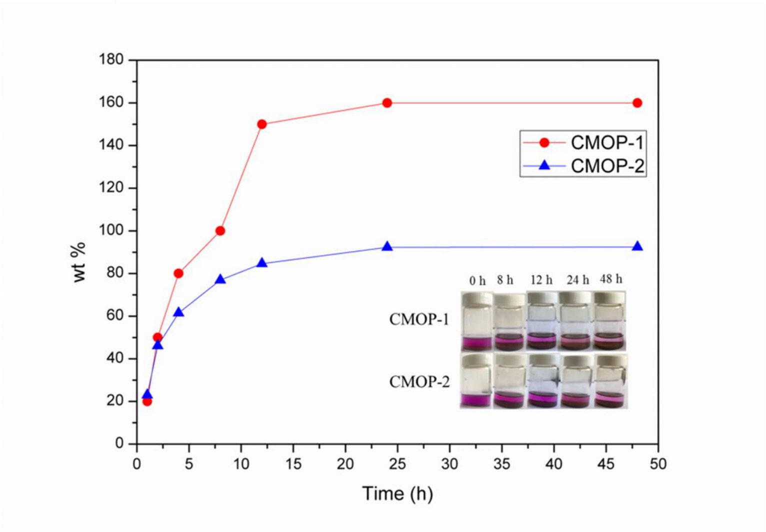

Figure 4. The uptake of I_2 vapor at 353 K.

3. Materials and Methods

3.1. General information

TEPT and azides were synthesized according to literature methods [38-40]. All of the other reagents were purchased from J&K (China) and used without further purification.

Before all of the measurement, polymers were dried under vacuum at 120 $^{\circ}C$ overnight. FTIR spectra were recorded on a Thermo-Nicolet iS10 spectrometer using KBr discs. Solid state ^{13}C CP-MAS NMR spectra data were collected on a BRUKER AVANCE III HD 400MHz NMR spectrometer. Element analysis for C, H and N were carried out with Elementar VarioMICRO Cube analyzer. Thermogravimetric analysis was performed on SDT Q600 V20.9 Build 20 with a temperature ramping rate of 10 $^{\circ}C\ min^{-1}$ from 30 to 850 $^{\circ}C$. Scanning electron microscopy (SEM) was performed on ZEISS Evo 18 scanning electron microscope at 20.0 KV. Powder X-ray diffraction (PXRD) data were recorded on Bruker D8 Advance, from 5° up to 35° with 4°/min increment. Nitrogen adsorption-desorption isotherms were carried out with a Demo 2020 instrument at 77 K. Carbon dioxide adsorption isotherms were measured at 273 and 298 K on 3Flex Version 4.02. Hydrogen adsorption isotherms were conducted at 77 K on Quadrasorb SI.

3.2. Synthesis

CMOP-1: Under nitrogen atmosphere, TEPT (80 mg, 0.209 mmol), azide-1 (51 mg, 0.318 mmol), $CuSO_4{\cdot}5H_2O$ (15 mg, 0.06 mmol), sodium ascorbate (13 mg, 0.05 mmol) and dry DMF (7 ml) were placed in flask, and then heated to reflux for 48 h. The resulting brown solid was filtrated and washed with water, methanol and DCM. The residue was stirred in distilled water overnight, and then filtrated and dried in vacuum (101 mg, 77%). Anal. calcd for $(C_{12}H_7N_4)_n$: C 69.54, H 3.41, N 27.04; found C 57.37, H 4.17, N 18.75.

CMOP-2: Under nitrogen atmosphere, TEPT (68 mg, 0.178 mmol), azide-2 (64 mg, 0.271 mmol), $CuSO_4{\cdot}5H_2O$ (14 mg, 0.05 mmol), sodium ascorbate (11 mg, 0.045 mmol) and dry DMF (7 ml) were placed in flask, and then heated to reflux for 48 h. The resulting brown solid was filtrated and washed with water, methanol and DCM. The residue was stirred in distilled water overnight, and then filtrated and dried in vacuum (106 mg, 80%). Anal. calcd for $(C_{15}H_9N_4)_n$: C 73.44, H 3.70, N 22.84; found C 63.20, H 4.27, N 15.49.

3.3 The gravimetric sorption of I_2 vapor

Peer-reviewed version available at *Molecules* **2018**, *23*, 1732; doi:10.3390/molecules23071732

10 mg of polymer was placed in an open bottle (10 ml) and weighted the total weight (W_0, mg). The open bottle was then putted into a sealed vessel (50 ml) which contained 200 mg of iodine at 353 K in the oil bath. The open bottle was taken out and weighted after 1, 4, 8, 12, 24 and 48 h (W_i, mg), respectively. The gravimetric sorption (wt%) was calculated using the following formula:

$$\text{wt\%} = (W_i - W_0) / 10 \times 100\%$$

4. Conclusions

In conclusion, we synthesized two nitrogen-rich and thermal stable microporous organic polymers by the condensation of 2,4,6-tris(4-ethynylphenyl)-1,3,5-triazine building block and aromatic azides linkers for the first time. Despite of the moderate surface areas of 431 and 406 $m^2\ g^{-1}$ based on nitrogen adsorption, CMOPs exhibited high CO_2 sorption and moderate H_2 sorption capacity, comparable or superior than many POPs with similar surface area. We ascribed the excellent CO_2 sorption capacity to nitrogen-rich content which improved the dipole-quadruple interaction between CO_2 and polymers. Furthermore, the CMOPs displayed significant gravimetric uptake ability toward I_2 vapor up to 160 wt%. The successfully constructed networks confirmed the advantage of nitrogen atom for the gas capture and inspired our great interest to explore more functional MOPs.

Acknowledgments: The authors thank Junmin Liu for gas sorption measurement. Financial supports from Fundamental Research Fund of Guangxi Institute of Botany (No. 16002) and the Director of Capital Projects of Guangxi Key Laboratory of Functional Phytochemicals Research and Utilization (No. ZRJJ2016-2) are acknowledged.

Author Contributions: J. S. conceptualized and designed the experiment route, performed all of the experiment work, participated in the discussion of result and wrote the paper. W. D. and D. L. supervised the work and discussed the result.

Conflicts of Interest: The authors declare no conflict of interest.

Sample Availability: Samples of the compounds are available from the authors.

References

1. Wang, C.-A.; Wang, W. Advances in Porous Organic Catalysis. *Acta Chim. Sinica* **2015**, *73*, 498-529.
2. Wang, W.; Zhou, M.; Yuan, D. Carbon dioxide capture in amorphous porous organic polymers. *J. Mater. Chem. A* **2017**, *5*, 1334-1347.
3. Kato, R.; Nishide, H. Polymers for carrying and storing hydrogen. *Polym. J.* **2018**, *50*, 77-82.
4. Lin, Y.; Zhu, Y.; Kuang, G.; Yu, G.; Jin, R. Application of porous organic polymers in the radioactive iodine adsorption. *Prog. Chem.* **2017**, *29*, 766-775.
5. Bai, L.; Phua, S. Z. F.; Lim, W. Q.; Jana, A.; Luo, Z.; Tham, H. P.; Zhao, L.; Gao, Q.; Zhao, Y. Nanoscale covalent organic frameworks as smart carriers for drug delivery. *Chem. Commun.* **2016**, *52*, 4128-4131.
6. Fang, Q.; Wang, J.; Gu, S.; Kaspar, R. B.; Zhuang, Z.; Zheng, J.; Guo, H.; Qiu, S.; Yan, Y. 3D Porous Crystalline Polyimide Covalent Organic Frameworks for Drug Delivery. *J. Am. Chem. Soc.* **2015**, *137*, 8352-8355.
7. Bai, L.; Gao, Q.; Zhao, Y. Two fully conjugated covalent organic frameworks as anode materials for lithium ion batteries. *J. Mater. Chem. A* **2016**, *4*, 14106-14110.
8. He, Q.; Zhang, C.; Li, X.; Wang, X.; Pan, M.; Jiang, J. Pyrene-Based Conjugated Microporous Polymer as High Performance Electrode for Lithium-Ion Batteries. *Acta Chim. Sinica* **2018**, *76*, 202-208.
9. Liu, X.; Xu, Y.; Jiang, D. Conjugated Microporous Polymers as Molecular Sensing Devices: Microporous Architecture Enables Rapid Response and Enhances Sensitivity in Fluorescence-on and Fluorescence-off Sensing. *J. Am. Chem. Soc.* **2012**, *134*, 8738-8741.
10. Ding, S.-Y.; Wang, W. Covalent organic frameworks (COFs): from design to applications. *Chem. Soc. Rev.* **2013**, *42*, 548-568.
11. Sakaushi, K.; Antonietti, M. Carbon- and Nitrogen-Based Porous Solids: A Recently Emerging Class of Materials. *Bull. Chem. Soc. Jpn.* **2015**, *88*, 386-398.

12. Rabbani, M. G.; El-Kaderi, H. M. Synthesis and Characterization of Porous Benzimidazole-Linked Polymers and Their Performance in Small Gas Storage and Selective Uptake. *Chem. Mater.* **2012**, *24*, 1511-1517.
13. Lu, W.; Yuan, D.; Zhao, D.; Schilling, C. I.; Plietzsch, O.; Muller, T.; Bräse, S.; Guenther, J.; Blümel, J.; Krishna, R.; Li, Z.; Zhou, H.-C. Porous Polymer Networks: Synthesis, Porosity, and Applications in Gas Storage/Separation. *Chem. Mater.* **2010**, *22*, 5964-5972.
14. Tan, L.; Tan, B. Hypercrosslinked porous polymer materials: design, synthesis, and applications. *Chem. Soc. Rev.* **2017**, *46*, 3322-3356.
15. Xu, Y.; Jin, S.; Xu, H.; Nagai, A.; Jiang, D. Conjugated microporous polymers: design, synthesis and application. *Chem. Soc. Rev.* **2013**, *42*, 8012-8031.
16. McKeown, N. B.; Bud, P. M. Polymers of intrinsic microporosity (PIMs): organic materials for membrane separations, heterogeneous catalysis and hydrogen storage. *Chem. Soc. Rev.* **2006**, *35*, 675-683.
17. Li, L.; Ren, H.; Yuan, Y.; Yu, G.; Zhu, G. Construction and adsorption properties of porous aromatic frameworks via $AlCl_3$-triggered coupling polymerization. *J. Mater. Chem. A* **2014**, *2*, 11091-11098.
18. Klumpen, C.; Radakovitsch, F.; Jess, A.; Senker, J. BILP-19-An Ultramicroporous Organic Network with Exceptional Carbon Dioxide Uptake. *Molecules* **2017**, *22*, 1343-1353.
19. Chen, Q.; Luo, M.; Hammershøj, P.; Zhou, D.; Han, Y.; Laursen, B. W.; Yan, C.-G.; Han, B.-H. Microporous Polycarbazole with High Specific Surface Area for Gas Storage and Separation. *J. Am. Chem. Soc.* **2012**, *134*, 6084-6087.
20. Yang, X.; Yu, M.; Zhao, Y.; Zhang, C.; Wang, X.; Jiang, J.-X. Remarkable gas adsorption by carbonized nitrogen-rich hypercrosslinked porous organic polymers. *J. Mater. Chem. A* **2014**, *2*, 15139-15145.
21. Wang, T.; Zhao, Y.-C.; Zhang, L.-M.; Cui, Y.; Zhang, C.-S.; Han, B.-H. Novel approach to hydroxy-group-containing porous organic polymers from bisphenol A. *Beilstein J. Org. Chem.* **2017**, *13*, 2131-2137.
22. Das, S. K.; Wang, X.; Lai, Z. Facile synthesis of triazine-triphenylamine-based microporous covalent polymer adsorbent for flue gas CO_2 capture. *Microporous Mesoporous Mat*. **2018**, *255*, 76-83.
23. Shao, L.; Li, Y.; Huang, J.; Liu, Y.-N. Synthesis of Triazine-Based Porous Organic Polymers Derived N‑Enriched Porous Carbons for CO_2 Capture. *Ind. Eng. Chem. Res.* **2018**, *57*, 2856-2865.
24. Puthiaraj, P.; Lee, Y.-R.; Zhang, S.; Ahn, W.-S. Triazine-based covalent organic polymers: design, synthesis and applications in heterogeneous catalysis. *J. Mater. Chem. A* **2016**, *4*, 16288-16311.
25. Wu, S.; Gu, S.; Zhang, A.; Yu, G.; Wang, Z.; Jian, J.; Pan, C. A rational construction of microporous imidebridged covalent–organic polytriazines for highenthalpy small gas absorption. *J. Mater. Chem. A* **2015**, *3*, 878-885.
26. Song, W.-C.; Xu, X.-K.; Chen, Q.; Zhuang, Z.-Z.; Bu, X.-H. Nitrogen-rich diaminotriazine-based porous organic polymers for small gas storage and selective uptake. *Polym. Chem.* **2013**, *4*, 4690-4696.
27. Hug, S.; Stegbauer, L.; Oh, H.; Hirscher, M.; Lotsch, B. V. Nitrogen-Rich Covalent Triazine Frameworks as High-Performance Platforms for Selective Carbon Capture and Storage. *Chem. Mater.* **2015**, *27*, 8001-8010.
28. Buyukcaki, O.; Je, S. H.; Talapanen, S. N.; Kim, D.; Coskun, A.; Charged Covalent Triazine Frameworks for CO_2 Capture and Conversion. *ACS Appl. Mater. Interfaces* **2017**, *9*, 7209-7216.
29. Hug, S.; Mesch, M. B.; Oh, H.; Popp, N.; Hirscher, M.; Senker, J.; Lotsch, B. V. A fluorene based covalent triazine framework with high CO_2 and H_2 capture and storage capacities. *J. Mater. Chem. A* **2014**, *2*, 5928-5936.
30. Tao, L.; Niu, F.; Liu, J.; Wang, T.; Wang, Q. Troger's base functionalized covalent triazine frameworks for CO2 capture. *RSC Adv.* **2016**, *6*, 94365-94372.
31. Tao, L.; Niu, F.; Wang, C.; Liu, J.; Wang, T.; Wang, Q. Benzimidazole functionalized covalent triazine frameworks for CO_2 capture. *J. Mater. Chem. A* **2016**, *4*, 11812-11820.
32. Weng, J.-Y.; Xu, Y.-L.; Song, W.-C.; Zhang, Y.-H. Tuning the Adsorption and Fluorescence Properties of Aminal-Linked Porous Organic Polymers through N-Heterocyclic Group Decoration. *J. Polym. Sci. Pol. Chem*. **2016**, *54*, 1724-1730.
33. Geng, T.; Ye, S.; Zhu, Z.; Zhang, W. Triazine-based conjugated microporous polymers with N,N,N′,N′-tetraphenyl-1,4-phenylenediamine, 1,3,5-tris(diphenylamino)benzene and 1,3,5-tris[(3-methylphenyl)-phenylamino]benzene as the core for high iodine capture and fluorescence sensing of o-nitrophenol. *J. Mater. Chem. A* **2018**, *6*, 2808-2816.
34. Sun, X.; Qi, Y.; Li, J.; Wang, W.; Ma, Q.; Liang, J. Ferrocene-linked porous organic polymers for carbon dioxide and hydrogen sorption. *J. Organomet. Chem.* **2018**, *859*, 117-123.

35. Chen, D.; Fu, Y.; Yu, W.; Yu, G.; Pan, C. Versatile Adamantane-based porous polymers with enhanced microporosity for efficient CO2 capture and iodine removal. *Chem. Eng. J.* **2018**, *334*, 900-906.
36. Zhang, R.-R.; Yin, Q.; Liang, H.-P.; Chen, Q.; Luo, W.-H. Hypercrosslinked porous polycarbazoles from carbazolyl-bearing aldehydes or ketones. *Polymer* **2018**, *143*, 87-95.
37. Neti, V. S. P. K.; Wu, X.; Deng, S.; Echegoyen, L. Selective CO_2 capture in an imine linked porphyrin porous polymer. *Polym. Chem.* **2013**, *4*, 4566-4569.
38. Jian, Z. A nanoporous organic polymer constructed from a 1,3,5-triazine derivative via ethynyl cyclotrimerization reaction: Synthesis and carbon dioxide capture. *J. Chem. Pharm. Res.* **2014**, *6*, 322-326.
39. Li, D.; Wang, X.; Jia, Y.; Wang, A.; Wu, Y. Synthesis of Conjugated Hyperbranched Polytriazoles Containing Truxene Units by Click Polymerization. *Chin. J. Chem.* **2012**, *30*, 861-868.
40. Wang, Y.; Wang, D.; Xu, C.; Wang, R.; Han, J.; Feng, S. Click polymerization: Synthesis of Novel σ-π Conjugated Organosilicon Polymers. *J. Organomet. Chem.* **2011**, *696*, 3000-3005.